

# LangPrecip: Language-Aware Multimodal Precipitation Nowcasting

Xudong Ling <sup>\*1</sup> Tianxi Huang <sup>2</sup> Qian Dong <sup>1</sup> Tao He <sup>1</sup> Chaorong Li <sup>\*3</sup> Guiduo Duan <sup>\*1</sup>

## Abstract

Short-term precipitation nowcasting is an inherently uncertain and under-constrained spatiotemporal forecasting problem, especially for rapidly evolving and extreme weather events. Existing generative approaches rely primarily on visual conditioning, leaving future motion weakly constrained and ambiguous. We propose a language-aware multimodal nowcasting framework (LangPrecip) that treats meteorological text as a semantic motion constraint on precipitation evolution. By formulating nowcasting as a semantically constrained trajectory generation problem under the Rectified Flow paradigm, our method enables efficient and physically consistent integration of textual and radar information in latent space. We further introduce LangPrecip-160k, a large-scale multimodal dataset with 160k paired radar sequences and motion descriptions. Experiments on Swedish and MRMS datasets show consistent improvements over state-of-the-art methods, achieving over 60 % and 19% gains in heavy-rainfall CSI at an 80-minute lead time.

## 1. Introduction

Accurate short-term precipitation nowcasting is a critical component of disaster prevention and early warning systems. Recent advances in probabilistic generative models, including diffusion models (Ho et al., 2020) and rectified flow (Liu et al., 2022; Lipman et al., 2022), have substantially improved nowcasting performance by modeling the full distribution of future radar fields, enabling both uncertainty representation and diverse forecasts. Representative approaches, such as DGMR (Ravuri et al., 2021a), DiffCast (Yu et al., 2024), and latent diffusion-based methods (Gao et al., 2023;

<sup>1</sup>Laboratory of Intelligent Collaborative Computing, University of Electronic Science and Technology of China (UESTC), Chengdu 611731 <sup>2</sup>College of Humanities and General Education, Chengdu Textile College, Chengdu 611731, China <sup>3</sup>School of Computer Science and Technology (School of Artificial Intelligence), Yibin University, Yibin 644000. Correspondence to: Guiduo Duan <duanguiduo@163.com>.

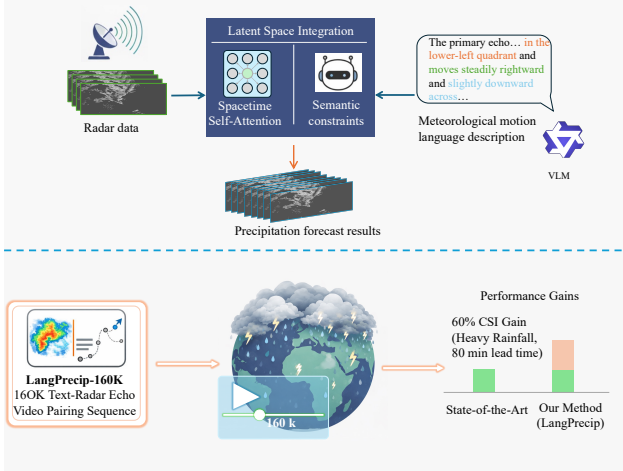


Figure 1. Overview of the proposed LangPrecip framework. Radar echo sequences are first encoded into a latent space, where spatiotemporal self-attention captures visual dynamics while semantic motion descriptions provide high-level constraints on precipitation evolution. The two streams are integrated in the latent space to guide future trajectory generation. Leveraging the LangPrecip-160K text–radar paired dataset, the model produces temporally coherent forecasts and achieves substantial performance gains, particularly for heavy precipitation events at long lead times.

Ling et al., 2024b; Li et al., 2024), have demonstrated strong performance across multiple benchmarks.

Despite these advances, existing generative nowcasting methods remain fundamentally limited in how motion is conditioned. Most approaches rely exclusively on historical visual observations (e.g., radar or satellite imagery), forcing models to infer future motion patterns implicitly from pixel-level variations. This formulation is inherently under-constrained in rapidly evolving or chaotic weather scenarios, particularly for sparse and extreme precipitation events, where multiple plausible motion trajectories are consistent with the same visual history. From a modeling perspective, meteorological motion descriptions provide a compact semantic abstraction of precipitation dynamics, which helps regularize this otherwise under-constrained solution space. Accordingly, we argue that short-term precipitation nowcasting should be viewed as a semantically constrained generative trajectory modeling problem, rather than a purely visual prediction task.

Notably, meteorological motion descriptions are routinely used in operational meteorology to characterize precipitation evolution, including propagation, deformation, and structural changes. However, in contrast to recent progress in text-guided visual generation (Wan et al., 2025; Zheng et al., 2024), such semantic motion information has yet to be systematically integrated as a generative constraint in short-term precipitation nowcasting.

In this work, we propose **LangPrecip**, a **language-aware multimodal precipitation nowcasting** framework that treats (as shown in Fig. 1) meteorological motion descriptions as semantic motion priors for future radar evolution. By formulating precipitation forecasting as a semantically constrained trajectory generation problem under the Rectified Flow paradigm, LangPrecip explicitly integrates textual motion cues with spatiotemporal radar dynamics, enabling more physically consistent and controllable forecasts.

In summary, our contributions are threefold:

- We construct Nowcast-VT, the first large-scale paired meteorological text–radar dataset for short-term precipitation nowcasting, comprising 130k video–text samples, and introduce a text-guided multimodal generative framework for this task.
- We formulate precipitation nowcasting as a semantically constrained trajectory generation problem under the Rectified Flow paradigm, enabling explicit integration of meteorological motion semantics beyond purely visual conditioning.
- Extensive experiments on the Swedish and MRMS benchmarks demonstrate consistent improvements in event-based and spatial metrics, particularly for heavy precipitation, while maintaining competitive uncertainty and structural fidelity.

## 2. Related Work

### 2.1. Deep Learning for Precipitation Nowcasting

Early deep learning approaches treat precipitation nowcasting as deterministic spatiotemporal sequence prediction. Representative models such as ConvLSTM (Shi et al., 2015) and Transformer-based architectures like Earthformer (Gao et al., 2022; Wang et al., 2025b) improve spatiotemporal modeling capacity, but their deterministic training objectives often lead to over-smoothed forecasts and limited uncertainty representation. To address the inherent stochasticity of precipitation evolution, recent work has adopted generative modeling paradigms. DGMR (Ravuri et al., 2021a) introduces adversarial learning for probabilistic nowcasting, while diffusion-based methods such as SSLDM-ISI (Ling et al., 2024b) and DTCA (Li et al., 2024) further enhance

distribution modeling and temporal coherence.

### 2.2. Text-Guided Video Generation and Multimodal Meteorology

Text-guided video generation models, including Imagen Video (Ho et al., 2022), Video LDM (Wang et al., 2025c), and recent Sora-like architectures (Ma et al., 2025; Peng et al., 2025), demonstrate that linguistic descriptions can effectively guide spatiotemporal dynamics through cross-modal attention mechanisms. In meteorology, recent benchmarks and datasets such as ChaosBench (Nathaniel et al., 2024) for subseasonal-to-seasonal climate prediction and Terra (Chen et al., 2024) for multimodal meteorological data focus on macro-scale climate variables or general representation learning, rather than the fine-grained radar echo dynamics required for precipitation nowcasting.

In summary, while existing precipitation nowcasting methods achieve strong performance through visual-only modeling, they lack high-level semantic guidance for motion and structure. Although text-guided generation has proven effective in video synthesis, language remains largely unexplored in fine-grained weather forecasting. We bridge this gap by leveraging meteorological motion descriptions as semantic constraints to guide radar echo evolution.

## 3. Method

### 3.1. LangPrecip-160K: A Multimodal Precipitation Nowcasting Dataset

We construct LangPrecip-160K (Fig. 2), a large-scale multimodal precipitation nowcasting dataset comprising approximately 160,000 events from two regions: 100,000 events from the Swedish SWish dataset and 60,000 events from the MRMS dataset. Each event consists of 20 radar echo frames with a temporal resolution of 5 minutes, covering 100 minutes in total. Each event is paired with a meteorological motion description that provides a high-level semantic summary of precipitation evolution; during training, this description is associated with the full 20-frame sequence, while during inference it is obtained solely from the first four observed frames to ensure a causal forecasting setup. We evaluate LangPrecip on the SWish and MRMS benchmarks (1,000 test events each) using four input frames to predict sixteen future frames, with standard precipitation thresholds (0.06/6.3 mm/h for SWish and 1/8 mm/h for MRMS) (Ling et al., 2024b; Ravuri et al., 2021a).

Approximately 30,000 events are manually annotated with high-quality motion descriptions, while the remaining events are annotated using a vision–language model (QWEN-3) with meteorology-specific prompts. A subset of the automatically generated descriptions is manually inspected to verify consistency with the underlying precipi-

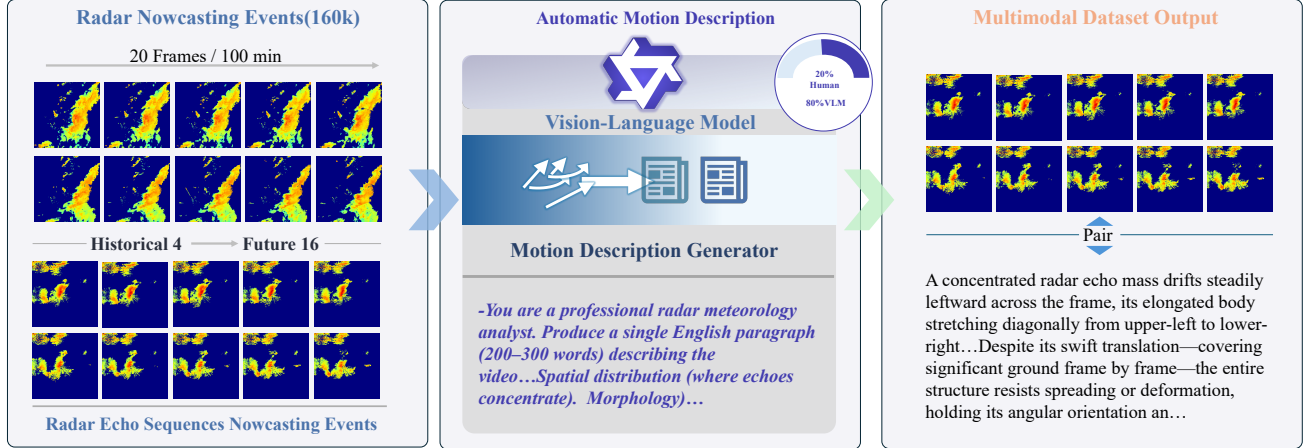


Figure 2. LangPrecip-160K dataset construction pipeline.

tation motion patterns. These motion descriptions capture coarse-grained and temporally aggregated dynamics (e.g., dominant propagation direction and structural evolution) and are treated as high-level semantic motion priors that complement radar-based visual inputs rather than direct observational measurements.

### 3.2. Semantically Constrained Rectified Flow

We formulate short-term precipitation nowcasting as a *semantically constrained trajectory generation* problem in latent space. Given historical radar observations, multiple future precipitation trajectories may be physically plausible, especially under rapidly evolving or extreme weather conditions. Our goal is to constrain this trajectory space using high-level motion semantics provided by meteorological language, while preserving the ability to model uncertainty.

To this end, we adopt the flow matching framework (Lipman et al., 2022) as an efficient and principled generative paradigm for modeling continuous trajectories. Rectified Flow models continuous trajectory dynamics via a deterministic velocity field that transports samples from a simple prior distribution to the target data distribution, making it well suited for incorporating semantic constraints on trajectory evolution.

Specifically, we operate on latent representations of radar sequences encoded by a variational autoencoder (VAE). Within this latent space, semantic motion information is incorporated as a constraint on trajectory evolution together with historical radar context, allowing high-level motion semantics to directly influence the generative dynamics rather than acting as a purely auxiliary signal.

### 3.3. Training Objective

We encode radar sequences using a 2D variational autoencoder (VAE) that downsamples the original radar fields of size  $256 \times 256$  by a factor of 8, producing latent representations of spatial size  $32 \times 32$ . All forecasting is performed entirely in this latent space by learning a Rectified Flow model conditioned on historical radar context ( $T = 4$ ) and meteorological motion descriptions. The predicted latent trajectories are decoded by the VAE decoder to obtain future radar sequences ( $T = 16$ ).

Given a target latent variable  $x_1$  and a Gaussian noise sample  $x_0 \sim \mathcal{N}(0, I)$ , rectified flow defines an interpolation

$$x_t = tx_1 + (1 - t)x_0, \quad (1)$$

with the corresponding ground-truth velocity

$$v_t = x_1 - x_0. \quad (2)$$

The model is trained via velocity regression by minimizing the mean squared error

$$\mathcal{L} = \mathbb{E}_{x_0, x_1, c_{\text{ctx}}, t} \|u(x_t, c_{\text{ctx}}, t; \theta) - v_t\|^2, \quad (3)$$

where  $u(\cdot)$  denotes the learned velocity field parameterized by  $\theta$ .

The conditioning context is defined as  $c_{\text{ctx}} = \{X_{0:4}, m\}$ , where  $X_{0:4}$  are encoded historical radar features and  $m$  is a motion description providing high-level semantic constraints on future precipitation transport. During training, motion descriptions are extracted from full 20-frame radar sequences to capture long-range dynamics, while at inference time only descriptions derived from the first four observed frames are used to ensure causal forecasting. Radar inputs are encoded using the same VAE encoder as the target latents, and motion descriptions are embedded using a T5-XXL(Chung et al., 2024) text encoder with a maximum

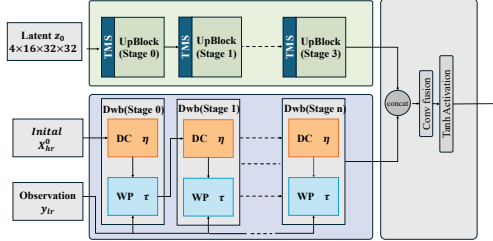


Figure 3. The decoder uses a dual-path design that combines UpBlocks with Temporal Shift Modules for cross-frame alignment and wavelet-based unfolding blocks for data-consistent refinement, followed by feature fusion to produce the final output.

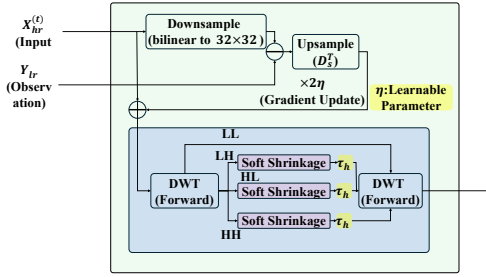


Figure 4. The Wavelet Consistency Unfolding Block (WCUB) consists of a data-consistency module for gradient updates and a wavelet-prior module that applies soft shrinkage to high-frequency coefficients for detail restoration.

length of 120 tokens. By jointly conditioning on visual context and motion semantics, the learned dynamics are guided toward physically consistent precipitation trajectories.

### 3.4. Wavelet Consistency Unfolding Decoder

We consider the reconstruction of a high-resolution image  $x$  from a low-resolution observation  $y$ , generated by blurring with kernel  $k$  followed by downsampling  $D_s(\cdot)$ :

$$y = D_s(x * k) + n, \quad (4)$$

where  $n$  denotes additive noise. This process leads to a severely ill-posed inverse problem due to information loss and noise corruption. To address this challenge, we propose a *wavelet-consistency unfolding decoder* that integrates model-based priors with deep feature learning. As shown in Fig. 3, the decoder adopts a dual-path design, combining a hierarchical upsampling branch for global structure recovery and a cascaded wavelet-consistency branch for stage-wise data fidelity and detail refinement.

Reconstruction is formulated as a regularized optimization problem:

$$\hat{x} = \arg \min_x \|y - D_s(x * k)\|^2 + \lambda R(x), \quad (5)$$

where the first term enforces consistency with the observation and  $R(x)$  denotes a wavelet-domain sparsity prior.

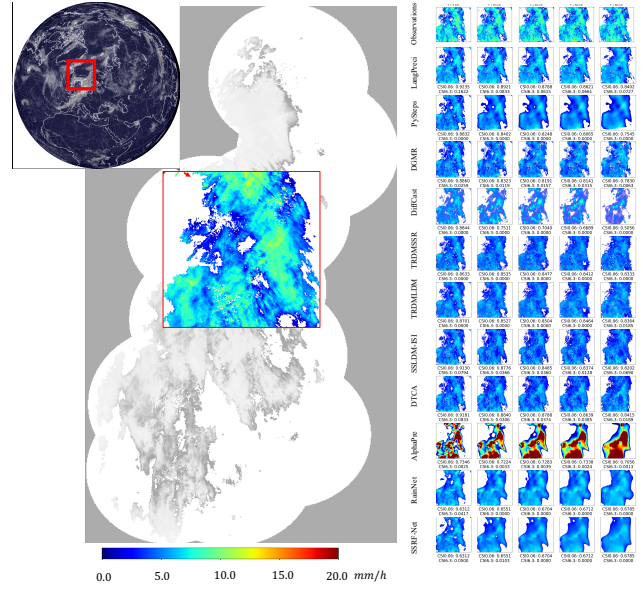


Figure 5. Spatial precipitation forecasts at multiple lead times (5-80 minutes) for different models with corresponding skill scores ( $CSI \geq 0.06 \text{ mm/h}$ ,  $CSI \geq 6.3 \text{ mm/h}$ ) during a Swedish weather event in Central Sweden (centered approximately at  $63.17^\circ\text{N}$ ,  $14.63^\circ\text{E}$ , in Östersund) on October 3, 2021, at 16:45.

We solve this problem via an iterative scheme, where each iteration performs a data-consistency update by back-projecting the residual:

$$x^{(t+1)} = x^{(t)} + 2\eta \cdot D_s^\top (y - D_s(x^{(t)} * k)). \quad (6)$$

The iterative process is unfolded into a  $T$ -stage deep network:

$$x^0 = U_s(y), \quad x^{t+1} = \mathcal{F}_{\theta_t}(x^t, y), \quad (7)$$

where each unfolding block  $\mathcal{F}_{\theta_t}$  consists of a data-consistency (DC) module followed by a wavelet prior (WP) module. As illustrated in Fig. 4, the DC module enforces observation fidelity through gradient-based back-projection, while the WP module applies wavelet-domain shrinkage to recover high-frequency details. The final reconstruction is obtained as  $\hat{x} = x^T$ . (Further implementation details are provided in Appendix ??.)

## 4. Results

### 4.1. Datasets and Experimental Setup

We compare our approach against representative baselines spanning optical-flow-based, GAN-based, diffusion-based, Transformer-based, and physics-guided methods, including PySteps, DGMR, DiffCast, SSLDM-ISI, DTCA, AlphaPre, RainNet, and SSRF-Net.

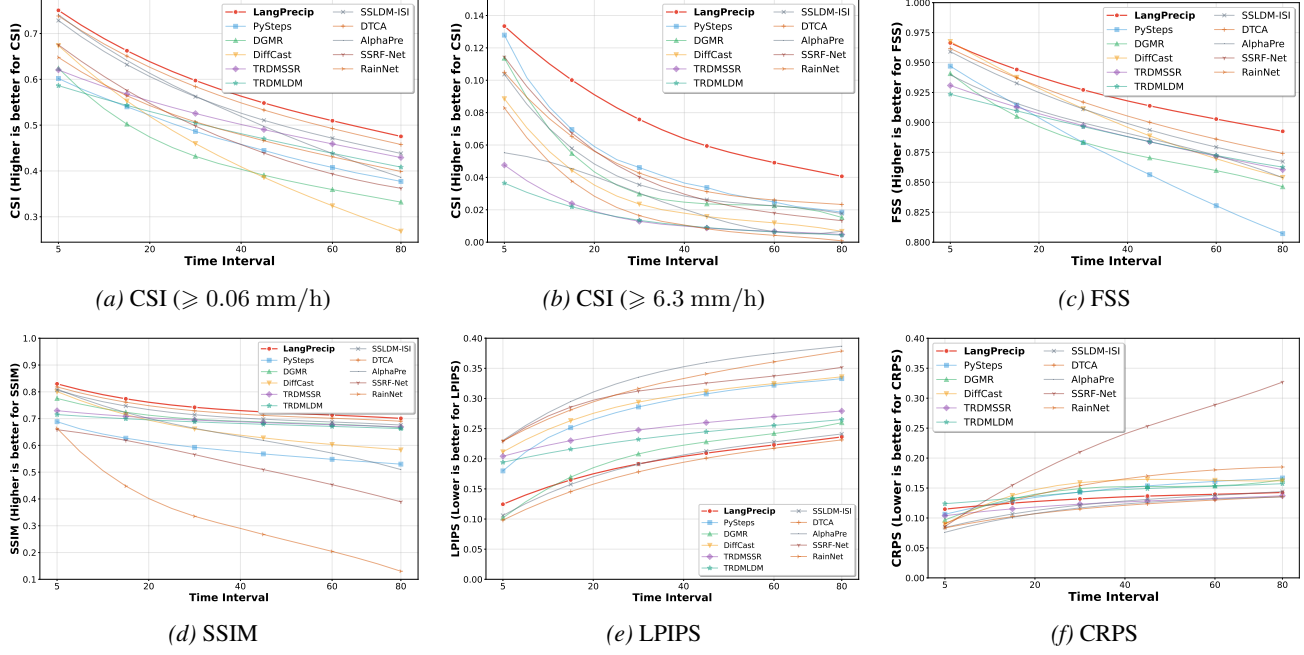


Figure 6. Temporal performance evolution on the Swedish dataset across lead times (5–80 minutes). All methods exhibit performance degradation as the prediction horizon increases.

Table 1. The average of all metrics in the Swedish Dataset with a lead time of 80 minutes (16 frames)

Method	$CSI \geq 0.06mm/h \uparrow$	$CSI \geq 6.3mm/h \uparrow$	$FSS \uparrow$	$CRPS \downarrow$	$SSIM \uparrow$	$LPIPS \downarrow$
PySteps(Pulkkinen et al., 2019)	0.473	0.049	0.872	0.144	0.589	0.284
DGMR(Ravuri et al., 2021b)	0.433	0.039	0.882	0.143	0.702	0.204
TRDM-SSR(Ling et al., 2024a)	0.513	0.015	0.892	0.123	0.693	0.249
TRDM-LSR(Ling et al., 2024a)	0.490	0.014	0.891	0.143	0.685	0.235
DiffCast(Yu et al., 2024)	0.439	0.029	0.903	0.149	0.660	0.292
SSLDM-ISI(Ling et al., 2024b)	0.558	0.040	0.906	0.122	0.718	0.191
AlphaPre(Lin et al., 2025)	0.541	0.025	0.894	0.149	0.647	0.333
DTCA(Li et al., 2024)	0.572	0.046	0.911	<b>0.115</b>	<b>0.732</b>	<b>0.180</b>
RainNet(Wang et al., 2025a)	0.499	0.025	0.386	0.153	0.332	0.207
SSRF-Net(Luo et al., 2025)	0.485	0.045	0.402	0.222	0.572	0.213
LangPreci(Ours)	<b>0.586</b>	<b>0.074</b>	<b>0.923</b>	0.132	<b>0.732</b>	0.193

## 4.2. A case study of precipitation forecasts

Fig.5 presents spatial precipitation forecasts at multiple lead times (5–80 minutes) for a representative Swedish weather event occurring at 16:45 on October 3, 2021, in central Sweden, centered approximately at  $63.17^\circ\text{N}$ ,  $14.63^\circ\text{E}$  (Östersund). From left to right, the figure compares predictions from different models against the corresponding observations across increasing forecast horizons, with skill scores reported under both light-precipitation ( $CSI \geq 0.06 \text{ mm/h}$ ) and heavy-precipitation ( $CSI \geq 6.3 \text{ mm/h}$ ) thresholds. As the lead time increases, most baseline methods exhibit pronounced structural degradation, including fragmented echoes, spatial diffusion, and mislocalized high-intensity cores. In contrast, LangPrecip consistently preserves the

global organization and coherent propagation of the precipitation system, maintaining more accurate localization of intense precipitation regions even at longer lead times. These visual results indicate that text-guided motion conditioning provides effective high-level constraints that stabilize spatial precipitation evolution and improve event detection performance.

## 4.3. Quantitative Results

Tables 1 and 2 report the quantitative results on the Swedish and MRMS datasets with an 80-minute lead time. The most pronounced benefit of text guidance appears in extreme precipitation detection. On the Swedish dataset, LangPreci improves heavy-precipitation  $CSI$  from 0.046

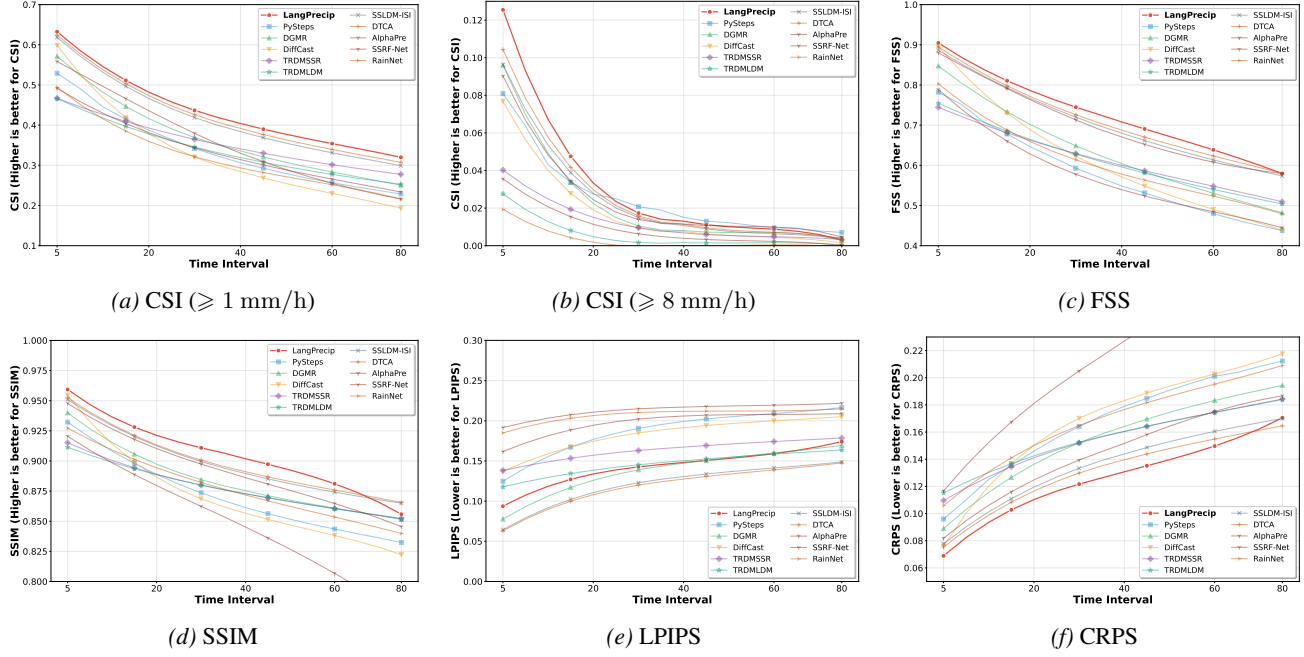


Figure 7. Temporal performance evolution on the MRMS dataset across lead times (5–80 minutes). All methods exhibit performance degradation as the prediction horizon increases.

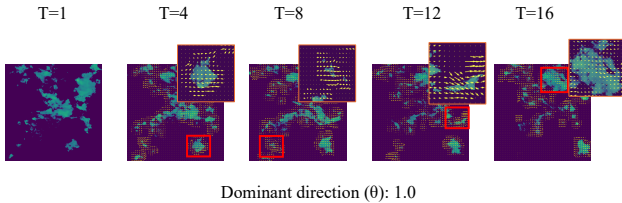
Table 2. The average of all metrics in the MRMS dataset with a lead time of 80 minutes (16 frames).

Method	CSI $\geq 1\text{mm}/\text{h}$ $\uparrow$	CSI $\geq 8\text{mm}/\text{h}$ $\uparrow$	FSS $\uparrow$	CRPS $\downarrow$	SSIM $\uparrow$	LPIPS $\downarrow$
PySteps(Pulkkinen et al., 2019)	0.338	0.024	0.579	0.167	0.871	0.187
DGMR(Ravuri et al., 2021b)	0.367	0.022	0.633	0.154	0.883	0.137
TRDM-SSR(Ling et al., 2024a)	0.356	0.012	0.614	0.154	0.877	0.163
TRDM-LSR(Ling et al., 2024a)	0.338	0.014	0.613	0.155	0.877	0.146
DiffCast(Yu et al., 2024)	0.328	0.018	0.613	0.168	0.869	0.183
SSLDM-ISI(Ling et al., 2024b)	0.416	0.024	0.704	0.135	0.897	0.120
AlphaPre(Lin et al., 2025)	0.360	0.024	0.699	0.144	0.891	0.197
DTCA(Li et al., 2024)	0.423	0.026	0.711	0.131	0.899	<b>0.118</b>
RainNet(Wang et al., 2025a)	0.320	0.002	0.606	0.153	0.877	0.207
SSRF-Net(Luo et al., 2025)	0.336	0.009	0.573	0.219	0.844	0.213
LangPreci(Ours)	<b>0.435</b>	<b>0.031</b>	<b>0.725</b>	<b>0.125</b>	<b>0.905</b>	0.142

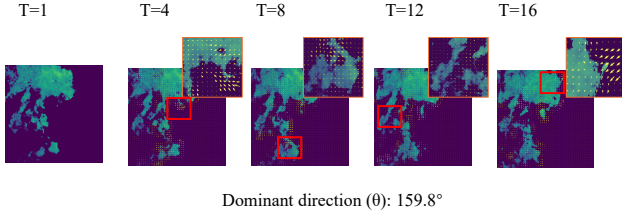
to 0.074, corresponding to a 60.9% relative gain, while on MRMS the improvement reaches 19.2% (0.026 to 0.031). In contrast, diffusion-based approaches (DGMR, TRDM, DiffCast) show substantial performance drops under high-intensity thresholds, with extreme-event CSI values below 0.04, trailing LangPreci by 50–80%. Notably, this degradation occurs despite these models producing visually coherent predictions ( $\text{SSIM} > 0.66$ ), indicating that reliance on visual cues alone is insufficient for modeling rare, high-intensity precipitation events. These results suggest that semantic motion guidance provides critical constraints that enhance sensitivity to extreme precipitation beyond what vision-only generative modeling can capture. Text descriptions encode meteorological context invisible in instantaneous radar frames—weather system types, development

stages, and physical processes. This contextual information enables LangPreci to make confident extreme predictions when meteorologically justified, rather than regressing toward conservative averages. The 60.9% gain on Swedish dataset is particularly striking: it suggests text provides qualitatively different information rather than incremental refinement of visual features.

Beyond extreme events, LangPreci achieves the best FSS (0.923 Swedish, 0.725 MRMS) and competitive CRPS, indicating superior spatial structure preservation and probabilistic calibration. DTCA obtains lower CRPS (0.115 vs 0.132 on Swedish) through visual attention, but at the cost of physical accuracy—it’s extreme event CSI lags by 60.9%. This trade-off suggests that optimizing perceptual metrics



(a) Prompt: *The radar echoes surge steadily **rightward** with near-perfect directional coherence, sweeping across the frame as fragmented ... no rupture, no collapse, only a stable, evolving dance of translation, spin, and squeeze, all choreographed by the larger atmospheric current guiding its path.*



(b) Prompt: *The radar echoes surge **leftward** and slightly **downward** in a swift, dragging their fragmented... frame—all motion locked to a single diagonal trajectory, unswerving, as if pulled by an invisible current through the sky.*

Figure 8. Dominant motion visualization of text-guided precipitation generation. Motion directions align with textual descriptions;  $0^\circ$  and  $90^\circ$  denote rightward and downward motion, respectively.

alone may not align with meteorological fidelity.

Figures 6 and 7 show all methods degrade with increasing lead time, but LangPreci maintains larger margins in CSI and FSS at longer horizons. This indicates that text-encoded temporal context (e.g., “rapidly developing system”) provides more robust extrapolation guidance than motion-based visual features.

#### 4.4. Motion Consistency Analysis

Beyond standard quantitative assessments, we further systematically examined whether the proposed language-aware multimodal framework can effectively perceive and regulate the spatiotemporal evolution of precipitation systems relying solely on textual motion descriptions. This experiment directly addresses a core issue in physical information generation modeling: whether high-level linguistic semantic abstraction can effectively and controllably constrain underlying physical dynamic processes.

In this experimental setup, we did not introduce any radar historical context as conditional input; instead, we explicitly used language as high-level semantic information to characterize the overall propagation direction, evolutionary trend, and structural changes of the precipitation system. This extreme setting, which removes visual priors, allows

Table 3. Effect of language conditioning with CFG on different evaluation metrics across two datasets.

Swedish Dataset				
CFG Setting	CRPS ( $\downarrow$ )	CSI $\geq 0.06$ ( $\uparrow$ )	CSI $\geq 6.3$ ( $\uparrow$ )	FSS ( $\uparrow$ )
No Text	0.1101	0.5668	0.0530	0.920
Text	0.1322	0.5869	0.0746	0.923
MRMS Dataset				
CFG Setting	CRPS ( $\downarrow$ )	CSI $\geq 1$ ( $\uparrow$ )	CSI $\geq 8$ ( $\uparrow$ )	FSS ( $\uparrow$ )
No Text	0.126	0.432	0.0302	0.7220
Text	0.125	0.435	0.0309	0.7258

for a clearer evaluation of the role and expressive power of linguistic semantics itself in guiding and constraining the spatiotemporal generation process.

To rigorously assess this language-to-dynamics alignment, we estimate dense optical flow between consecutive predicted radar frames and summarize the overall motion using the dominant direction, computed as the magnitude-weighted circular mean of flow orientations. This statistic captures the bulk advection behavior of the generated precipitation systems while remaining robust to local fluctuations. Angles are defined in image coordinates, where  $0^\circ$  denotes rightward motion and  $90^\circ$  denotes downward motion.

As illustrated in Fig. 8a, different textual motion descriptions induce clearly separable and semantically consistent dominant motion patterns in the generated precipitation videos. For example, a prompt describing coherent rightward propagation yields a dominant motion direction of  $1.0^\circ$ , whereas a prompt specifying leftward and downward movement results in a dominant direction of  $159.8^\circ$ . The resulting angular separation closely reflects the semantic contrast expressed in the prompts, indicating a systematic alignment between linguistic motion cues and geometric trajectories in physical space.

These observations suggest that the proposed method supports semantically guided and physically interpretable spatiotemporal dynamics, extending beyond purely pixel-wise prediction toward structured motion control. By imposing high-level language-aware motion constraints, the model promotes coherent precipitation propagation through global consistency, which complements local pattern modeling and provides a mechanistic explanation for the observed improvements in event-based and spatial metrics such as CSI and FSS. Overall, this demonstrates the potential of incorporating domain-relevant motion knowledge via natural language priors to enable more interpretable and controllable weather prediction.

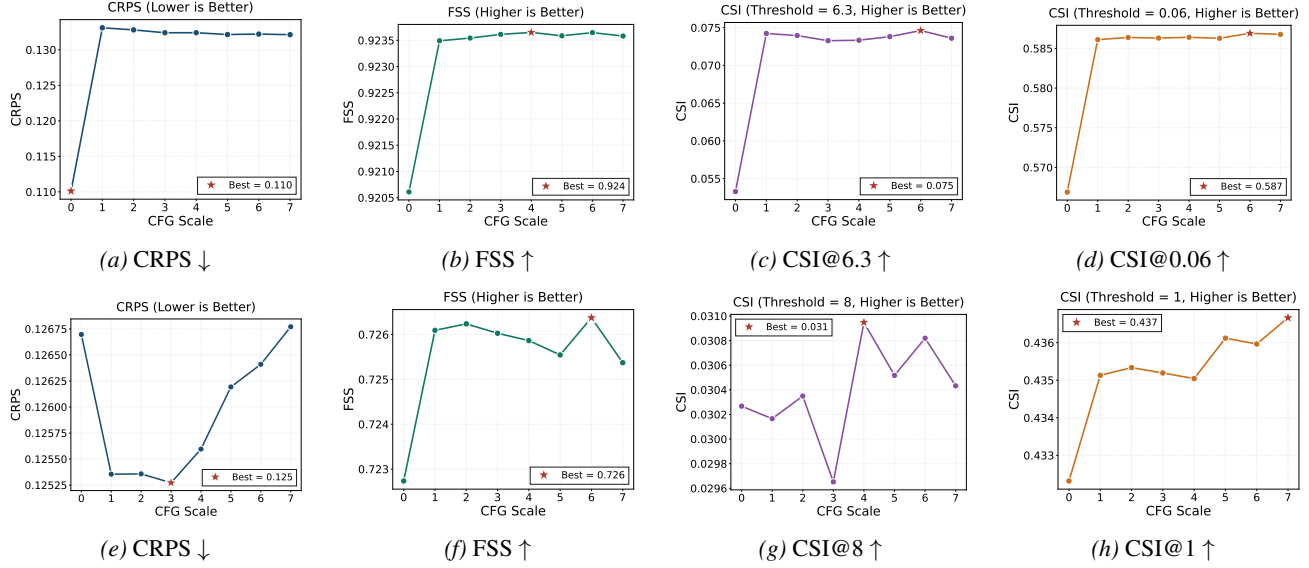


Figure 9. Effect of CFG scale on precipitation nowcasting performance. Top row: Swedish dataset. Bottom row: MRMS dataset. Event-based metrics (CSI) and spatial consistency (FSS) consistently improve with moderate CFG, while CRPS exhibits limited variation.

## 5. Ablation Experiment

### 5.1. Text scheduling degree

Figure 9 and Table 3 analyze the impact of motion text conditioning under different classifier-free guidance (CFG) scales on two precipitation nowcasting datasets. In this setting, CFG is used to modulate the relative strength of high-level semantic constraints provided by textual motion descriptions during generation. Following classifier-free guidance, the guided velocity (or score) is computed as

$$\hat{v}_{\text{CFG}}(x_t, c) = (1 + s) v(x_t, c) - s v(x_t, \emptyset),$$

where  $v(x_t, c)$  denotes the predicted velocity conditioned on the motion text  $c$ ,  $v(x_t, \emptyset)$  is the unconditional prediction, and  $s$  is the CFG scale controlling the strength of textual conditioning.

Overall, linguistic constraints substantially reshape the model’s prediction behavior across multiple aspects of forecast quality. On both datasets, textual guidance consistently improves event-oriented and structure-oriented metrics, including CSI and FSS, with particularly pronounced gains at higher precipitation thresholds.

On the Swedish dataset,  $\text{CSI} \geq 6.3$  increases by approximately 40% (from 0.0530 to 0.0746), while on the MRMS dataset,  $\text{CSI}@8$  shows a 2.3% improvement. These gains at high thresholds indicate that motion descriptions provide effective high-level structural priors—such as propagation direction, advection patterns, and morphological evolution—that help preserve precipitation organization and enhance event detection. In parallel, FSS exhibits consistent improvements (Swedish: 0.920→0.923; MRMS:

0.722→0.726), reflecting enhanced spatial coherence in the predicted precipitation fields. Together, these results suggest that textual conditioning improves the model’s ability to capture physically meaningful dynamics, especially in preserving the overall precipitation morphology and the spatial organization of heavy rainfall regions.

Table 4. Performance Comparison of Multi-stage VAE Training

Model	PSNR↑ (dB)	SSIM↑	FVD↓
2D Shift VAE (No Temporal Compression, WCUB)	<b>29.65</b>	<b>0.952</b>	<b>6.94</b>
2D VAE (No Temporal Compression, WCUB)	29.10	0.945	7.81
2D VAE with WCUB + Conv3D	29.10	0.945	8.03
2D VAE with WCUB + Conv3D ResBlock	21.77	0.753	131.13
2D VAE (No Temporal Compression)	28.78	0.943	9.18

### 5.2. Temporal Modeling and WCUB Design

To isolate decoder-side temporal modeling, we fix the 2D VAE encoder without temporal compression and evaluate different decoder designs (Table 4). Under this setting, the proposed WCUB consistently improves spatial reconstruction over the vanilla 2D VAE, and further gains are achieved by adding a lightweight time-shift module, yielding the best overall performance in PSNR, SSIM, and FVD. In contrast, directly introducing 3D convolutions or 3D residual blocks leads to unstable optimization and severe FVD degradation, indicating that heavy spatiotemporal modeling is inefficient when the encoder representation is fixed.

## 6. Conclusion and Future Work

**Conclusion:** In this work, we propose LangPrecip, a language-aware multimodal framework for short-term precipitation nowcasting that treats meteorological motion de-

scriptions as high-level semantic constraints on future precipitation evolution. By formulating nowcasting as a semantically constrained trajectory generation problem under the Rectified Flow paradigm, LangPrecip explicitly integrates radar observations with motion language in latent space, addressing the inherent under-constrained nature of purely visual forecasting. We further construct LangPrecip-160K, a large-scale paired radar–text dataset that supports effective multimodal training. Extensive experiments on the Swedish and MRMS benchmarks demonstrate that incorporating semantic motion priors consistently improves forecasting performance, particularly for long lead times and heavy precipitation events. These results suggest that language-guided motion modeling provides a promising direction for enhancing the robustness and physical consistency of precipitation nowcasting.

**Limitations and Future Work:** Despite the promising results, LangPrecip relies on the availability and quality of meteorological motion descriptions. In our current setting, a substantial portion of the text annotations are produced automatically, which may introduce noise or bias and potentially limit robustness under distribution shifts. Moreover, the motion descriptions mainly capture coarse-grained, temporally aggregated dynamics, and may be insufficient to fully represent fine-scale convective initiation, rapid intensification, or multi-cell interactions. Future work will explore more reliable and scalable ways to obtain motion semantics (e.g., expert-in-the-loop annotation, uncertainty-aware text generation, or learning motion tokens directly from observations), as well as richer language representations that better align with physically meaningful quantities.

## References

Chen, W., Hao, X., Wu, Y., and Liang, Y. Terra: A multimodal spatio-temporal dataset spanning the earth. In *Advances in Neural Information Processing Systems*, 2024.

Chung, H. W., Hou, L., Longpre, S., Zoph, B., Tay, Y., Fedus, W., Li, Y., Wang, X., Dehghani, M., Brahma, S., et al. Scaling instruction-finetuned language models. *Journal of Machine Learning Research*, 25(70):1–53, 2024.

Gao, Z., Shi, X., Wang, H., Zhu, Y., Wang, Y. B., Li, M., and Yeung, D.-Y. Earthformer: Exploring space-time transformers for earth system forecasting. *Advances in Neural Information Processing Systems*, 35:25390–25403, 2022.

Gao, Z., Shi, X., Han, B., Wang, H., Jin, X., Maddix, D., Zhu, Y., Li, M., and Wang, Y. B. Prediff: Precipitation nowcasting with latent diffusion models. *Advances in Neural Information Processing Systems*, 36:78621–78656, 2023.

Ho, J., Jain, A., and Abbeel, P. Denoising diffusion probabilistic models. *Advances in Neural Information Processing Systems*, 33:6840–6851, 2020.

Ho, J., Chan, W., Saharia, C., Whang, J., Gao, R., Gritsenko, A., Kingma, D. P., Poole, B., Norouzi, M., Fleet, D. J., et al. Imagen video: High definition video generation with diffusion models. *arXiv preprint arXiv:2210.02303*, 2022.

Li, C., Ling, X., Xue, Y., Luo, W., Zhu, L., Qin, F., Zhou, Y., and Huang, Y. Precipitation nowcasting using diffusion transformer with causal attention. *IEEE Transactions on Geoscience and Remote Sensing*, 2024.

Lin, K., Zhang, B., Yu, D., Feng, W., Chen, S., Gao, F., Li, X., and Ye, Y. Alphapre: Amplitude-phase disentanglement model for precipitation nowcasting. In *Proceedings of the Computer Vision and Pattern Recognition Conference*, pp. 17841–17850, 2025.

Ling, X., Li, C., Qin, F., Zhu, L., and Huang, Y. Two-stage rainfall-forecasting diffusion model. *IEEE Geoscience and Remote Sensing Letters*, 21:1–5, 2024a.

Ling, X., Li, C., Zhu, L., Qin, F., Zhu, P., and Huang, Y. Spacetime separable latent diffusion model with intensity structure information for precipitation nowcasting. *IEEE Transactions on Geoscience and Remote Sensing*, 2024b.

Lipman, Y., Chen, R. T., Ben-Hamu, H., Nickel, M., and Le, M. Flow matching for generative modeling. *arXiv preprint arXiv:2210.02747*, 2022.

Liu, X., Gong, C., and Liu, Q. Flow straight and fast: Learning to generate and transfer data with rectified flow. *arXiv preprint arXiv:2209.03003*, 2022.

Luo, W., Li, C., Ling, X., Deng, C., and Wang, Z. Ssrfnet: A stagewise scheduled rainfall forecasting network with an asymmetric architecture. *IEEE Transactions on Geoscience and Remote Sensing*, 63:1–18, 2025.

Ma, X., Wang, Y., Chen, X., Jia, G., Liu, Z., Li, Y.-F., Chen, C., and Qiao, Y. Latte: Latent diffusion transformer for video generation. *Transactions on Machine Learning Research*, 2025.

Nathaniel, J., Qu, Y., Nguyen, T., Yu, S., Busecke, J., Grover, A., and Gentine, P. Chaosbench: A multi-channel, physics-based benchmark for subseasonal-to-seasonal climate prediction. *arXiv preprint arXiv:2402.00712*, 2024.

Peng, X., Zheng, Z., Shen, C., Young, T., Guo, X., Wang, B., Xu, H., Liu, H., Jiang, M., Li, W., et al. Open-sora 2.0: Training a commercial-level video generation model in 200 k. *arXiv preprint arXiv:2503.09642*, 2025.

Pulkkinen, S., Nerini, D., Pérez Hortal, A. A., Velasco-Forero, C., Seed, A., Germann, U., and Foresti, L. Pysteps: An open-source python library for probabilistic precipitation nowcasting (v1. 0). *Geoscientific Model Development*, 12(10):4185–4219, 2019.

Ravuri, S., Lenc, K., Willson, M., Kangin, D., Lam, R., Mirowski, P., Fitzsimons, M., Athanassiadou, M., Kashem, S., Madge, S., et al. Skilful precipitation nowcasting using deep generative models of radar. *Nature*, 597(7878):672–677, 2021a.

Ravuri, S., Willson, M., and et al. Skilful precipitation nowcasting using deep generative models of radar. *Nature*, 597(7878):672–677, 2021b.

Shi, X., Chen, Z., Wang, H., Yeung, D.-Y., and Wong, W.-K. Convolutional lstm network: A machine learning approach for precipitation nowcasting. *Advances in neural information processing systems*, 28, 2015.

Wan, T., Wang, A., Ai, B., Wen, B., Mao, C., Xie, C.-W., Chen, D., Yu, F., Zhao, H., Yang, J., et al. Wan: Open and advanced large-scale video generative models. *arXiv preprint arXiv:2503.20314*, 2025.

Wang, L., Wang, Z., Hu, W., and Bai, C. Rainhcnnet: Hybrid high-low frequency and cross-scale network for precipitation nowcasting. *IEEE Journal of Selected Topics in Applied Earth Observations and Remote Sensing*, 2025a.

Wang, S., Sun, M., and Li, Y. Nowcasting echo top for aviation operations using cnn-transformer. *IEEE Transactions on Intelligent Transportation Systems*, 2025b.

Wang, Y., Chen, X., Ma, X., Zhou, S., Huang, Z., Wang, Y., Yang, C., He, Y., Yu, J., Yang, P., et al. Lavie: High-quality video generation with cascaded latent diffusion models. *International Journal of Computer Vision*, 133(5):3059–3078, 2025c.

Yu, D., Li, X., Ye, Y., Zhang, B., Luo, C., Dai, K., Wang, R., and Chen, X. Diffcast: A unified framework via residual diffusion for precipitation nowcasting. In *Proceedings of the IEEE/CVF Conference on Computer Vision and Pattern Recognition*, pp. 27758–27767, 2024.

Zheng, Z., Peng, X., Yang, T., Shen, C., Li, S., Liu, H., Zhou, Y., Li, T., and You, Y. Open-sora: Democratizing efficient video production for all. *arXiv preprint arXiv:2412.20404*, 2024.